

## Polysulfone–polyurethane (PSf-PUR) blend partly degradable hollow fiber membranes: preparation, characterization, and computer image analysis

Wioleta Sikorska<sup>a,\*</sup>, Cezary Wojciechowski<sup>a</sup>, Małgorzata Przytułska<sup>a</sup>, Gabriel Rokicki<sup>b</sup>,  
Monika Wasyleczko<sup>a</sup>, Juliusz L. Kulikowski<sup>a</sup>, Andrzej Chwojnowski<sup>a</sup>

<sup>a</sup>Department of Biomaterials and Biotechnological Systems, Nałęcz Institute of Biocybernetics and Biomedical Engineering, Polish Academy of Sciences, Trojdena 4 str., 02-109 Warsaw, Poland, emails: [wsikorska@ibib.waw.pl](mailto:wsikorska@ibib.waw.pl) (W. Sikorska), [cwojciechowski@ibib.waw.pl](mailto:cwojciechowski@ibib.waw.pl) (C. Wojciechowski), [mprzytulska@ibib.waw.pl](mailto:mprzytulska@ibib.waw.pl) (M. Przytułska), [mwasyleczko@ibib.waw.pl](mailto:mwasyleczko@ibib.waw.pl) (M. Wasyleczko), [jkulikowski@ibib.waw.pl](mailto:jkulikowski@ibib.waw.pl) (J.L. Kulikowski), [achwojnowski@ibib.waw.pl](mailto:achwojnowski@ibib.waw.pl) (A. Chwojnowski)  
<sup>b</sup>Faculty of Chemistry, Warsaw University of Technology, Nałkowskiego 3 str., 00-644 Warsaw, Poland, email: [gabro@ch.pw.edu.pl](mailto:gabro@ch.pw.edu.pl)

Received 7 June 2018; Accepted 27 August 2018

### ABSTRACT

In this study, the preparation of polysulfone (PSf)-polyurethane (PUR) partly degradable hollow fiber membranes is presented. The membrane forming solution was prepared by mixing two solutions: PSf in *N*-methyl-2-pyrrolidone (NMP) and PUR in NMP. The PSf-PUR membranes were received by dry/wet-spinning phase-inversion technique. The membranes were hydrolyzed with sodium hydroxide (NaOH) solution using the flowing method. The membranes were characterized by hydraulic permeability coefficient (UFC), retention coefficients, scanning electron microscopy (SEM) and mass measurement before and after hydrolysis. The changes in membranes morphology and properties due to hydrolysis were studied. Hydrolysis caused the partial removal of the PUR from the membrane structure resulting in the morphology change and the permeability's increase. The computer-aided image processing method was also used to investigate the morphology before and after the hydrolysis process. This method checked out the changes of membranes' morphology by the dissimilarity coefficient (values  $\neq 0$ ). The SEM images showed differences in structure of pores before and after the hydrolysis process. The structures and morphology of the membranes after hydrolysis were more porous. The hydraulic permeability coefficients were higher after the hydrolysis process. The retention coefficients were different before and after the hydrolysis process.

**Keywords:** Polysulfone–polyurethane blend hollow fiber membranes; Hydrolyzing; Fouling; Computer image analysis; Porosity evaluation

### 1. Introduction

Number of polymers are used as membrane fabrication materials, for example, cellulose acetate, polybenzimidazoles, polyamides, polyols, polyacrylonitrile, polysulfone (PSf), polyethersulfone, poly(tetrafluoroethylene), and polyvinylidene fluoride. There are several fabrication techniques, such as solution casting, solution wet-spinning, and electrospinning. Average pore size of membranes

depends on a fabrication technique applied and the type of used polymer [1].

Hydraulic stability and high thermal, mechanical, and chemical resistances are the advantages of PSf membranes. There are some disadvantages and the most important of these is fouling [2–4]. Fouling is a process of sticking of organic compounds to a surface and an inner structure of a membrane. It leads to an obstruction of membranes' pores. [5]. Because membranes are used in biotechnology, medicine, etc. [6–16], fouling is an important problem of their

\* Corresponding author.

Presented at the XII Scientific Conference "Membranes and Membrane Processes in Environmental Protection" – MEMPEP 2018 13–16 June 2018, Zakopane, Poland.

application. If a membrane is susceptible to fouling it is less productive and has to be exchanged by a new one.

There are several methods enabling the modification of the properties of membranes, such as sol-gel method, grafting, and cross-linking polymerization [17–22]. The most popular method for reducing or eliminating the fouling is the addition of a hydrophilic or biodegradable compound to membranes' casting solution in order to increase the hydrophilicity. Another way is the addition of a pore former (e.g., polyvinylpyrrolidone) [23–34].

The method of increasing hydrophilicity and reducing a fouling effect is presented in this study. The hydrophilic compound – polyurethane (PUR) was added to a membrane forming solution. The assumption was that PUR would be slowly hydrolyzed and partly removed from the membrane structure in water environment. Removal of the PUR would produce more porous and loosely knit structure of membranes that could compensate increasing fouling and extend time of their use. This type of membranes can be used for implantation, encapsulation, and biotechnology. The target of this study was also to search for new materials for biomedical engineering. In previous works, the compound such as cellulose acetate [32,33] and PUR [34] were presented. The difference between previous study [34] and this one lays in the structure of PURs. 1,5-Pentanediol was used for the synthesis of PUR in this work and 1,4-butanediol in the previous work. PURs with 1,5-pentanediol were amorphous, therefore PURs were better dissolved. PURs with 1,4-butanediol were more crystalline than other ones and had worse solubility, because of the symmetry of the structure. The change of chemical reagents was necessary for obtaining two solutions (of PSf and PUR) that provided a better solution and stirred up together. The obtained membranes were partially hydrolyzed by 1 M NaOH solution. After hydrolysis, the structures of the membranes were more porous and the hydraulic permeability increased.

Scanning electron microscope (SEM) was used for analyzing the morphology of membranes. The pictures showed changes in the porosity and the morphology of the membranes before and after hydrolysis. The morphology of the membranes was also controlled by a comparative assessment based on porosity analysis for confirming the changes in the structure of the membranes. The statistic method was previously used for the analysis of 3-D scaffolds [35], but never for the analysis of the hollow fiber membranes.

Effects of hydrolysis consisting of changing size and shapes of pores need to be exactly controlled. The problem may occur because any measurable parameters describing individual pores should be considered as instances of random values rather than determined values. Thereby, any comparative evaluation of porosity of membranes under investigation should be based on statistical methods.

The materials provided for computer analysis were in the form of SEM images presenting sections of exemplary specimens of the membranes before and after hydrolysis. For reaching reliable results of evaluation of the effects of hydrolysis the following conditions should be fulfilled:

- The SEM images selected for analysis should be typical of the classes of membranes before and after hydrolysis.

- The number of images in both classes should be statistically representative.
- The quality of images should be sufficiently high.

A high quality of images means: noiseless, high-contrast, high-distinctive, free of artifacts, equalized mean brightness. In addition, there should be compared series of images of unified magnification presented in a unified scale. Reaching such image quality standard requires some preprocessing procedures before the proper operation of image analysis. In our case, the preliminary operations were performed using the MeMoExplorer [36] procedures selected for the given problem.

## 2. Experimental

### 2.1. Materials

PSf Udel 1700 NT LCD from Dow Corning, M.W. (molecular weight) 70 kDa; PUR (the synthesis of the PUR is presented in Fig. 1); *N*-methyl-2-pyrrolidone (NMP) from Fluka; polyethylene glycols (PEG) from Fluka, M.W. 4, 15, 35 kDa; chicken egg albumin (CEA) from Sigma-Aldrich, M.W. 45 kDa; bovine serum albumin (BSA) from Fluka, M.W. 67 kDa; sodium hydroxide (NaOH) from POCH; water 1.2 MΩcm from MilliQ installation.

### 2.2. Capillary membranes preparation

PSf and PUR were selected as materials for blend hollow fiber membranes preparation. NMP was used as a solvent for both polymers. PSf and PUR were mixed with NMP in two different flasks and stirred at 20°C temperature until complete dissolution. Received solutions were mixed in a flask for 24 h. The PSf:PUR weight ratios were: 9:1, 8:2, and 7:3. A concentration of the polymers in NMP solution was 17% of the total solution's weight. PUR and PSf created the blend. Therefore, it was possible to selectively remove the PUR from a membrane without destroying its structure, after the PSf-PUR membrane fabrication.

A dry/wet-spinning, phase inversion technique through an extrusion of the polymeric solution was a method of membranes' production. The membranes' formation was controlled by a software program enabling quick changes of the process parameters. The spinning process was conducted at a room temperature. The membranes were cut into small pieces and placed in the clean water bath for 3 d for residual solvent extraction. In the end, the membranes were air-dried at room temperature.

The capillary membrane modules were prepared by putting 25, 5.9-cm length pieces of capillaries into polypropylene modules (about 25.0 cm<sup>2</sup> area). Both ends of the modules were sealed with an epoxy resin. Three types of PSf-PUR membranes with different PSf-PUR weight ratio were obtained. The membranes were marked as PSf-PUR-1 (PSf:PUR 9:1), PSf-PUR-2 (PSf:PUR 8:2), and PSf-PUR-3 (PSf:PUR 7:3). After receiving the modules, the membranes were ready for further analysis.

### 2.3. Hydrolysis of membranes

PSf-PUR membranes were treated with a 1 M NaOH water solution using the flowing method. 1 dm<sup>3</sup> of NaOH solution was passed through the membrane's module from

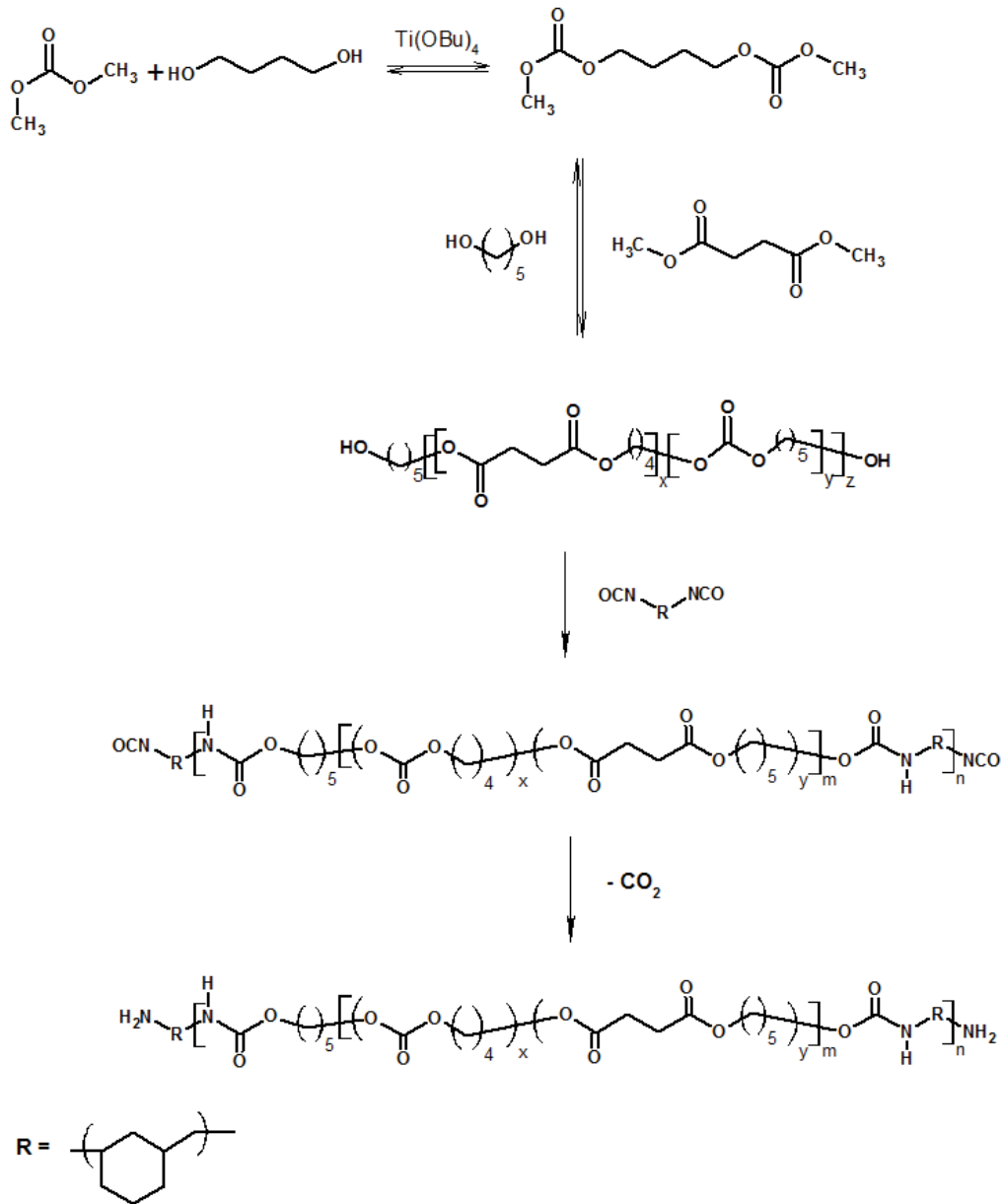


Fig. 1. The synthesis of the polyurethane.

inside of the capillaries, through the membrane’s walls to the outside of the module using the transmembrane pressure of 130 hPa. The hydrolysis process was conducted at room temperature (about 20°C) and lasted 48 h in all cases. After hydrolysis, demineralized water was passed through the membrane’s walls for removing sodium hydroxide and products of hydrolysis decomposition.

## 2.4. Characterization of the membranes

### 2.4.1. SEM analysis

The morphology of the prepared membranes was characterized by SEM, using a Hitachi TM-100 microscope. The samples for analysis were prepared by cutting the membranes in

liquid nitrogen for avoiding deformation during fracture. After cutting, the pieces of membranes were coated with a 10-nm gold layer, using a sputtering device (EMITECH K 550 X).

### 2.4.2. Permeability measurements

The hydraulic permeability of the capillaries was measured as a volume of pure water passed through the membrane’s walls during the period of 10 min under 200 hPa transmembrane pressure. The ultrafiltration coefficient (UFC) was calculated according to the following formula:

$$\text{UFC} = \frac{v}{t \times p \times a} \quad (1)$$

where  $v$  – the volume of pure water ( $\text{cm}^3$ );  $t$  – the time of measure (min);  $p$  – transmembrane pressure (hPa); and  $a$  – nominal membrane's area in a module ( $\text{m}^2$ ).

#### 2.4.3. Retention measurements

The retention coefficient is a measure of separation. The membrane retention (%) is defined as follows:

$$R = \left\{ 1 - \left( \frac{C_p}{C_f} \right) \right\} \times 100\% \quad (2)$$

where  $R$  – retention coefficient;  $C_p$  – concentration of a marker in permeate ( $\text{g}/\text{dm}^3$ ); and  $C_f$  – concentration of a marker in the feed ( $\text{g}/\text{dm}^3$ ).

PEG (4, 15, 35 kDa), CEA (45 kDa), and BSA (67 kDa) were successively used for the measurement of retention of all of the membrane's modules. The concentrations of markers ( $1 \text{ g}/\text{dm}^3$ ) were evaluated by a UV-spectrophotometer (HITACHI U-3010) at 190 nm wavelength for PEGs and 280 nm for CEA and BSA. The membrane modules were washed after each marker for 24 h and the membrane performance was controlled by UFC measurements after retention measurements.

#### 2.4.4. Comparative evaluation of porosity in membranes subjected to hydrolysis

MeMoExplorer is an original computer system designed for automation of the procedures of analysis of membrane

section images. It enables analysis of a single as well as a series of images. In particular, an image preprocessing and evaluation of morphometrical parameters used for membranes quality assessment by MeMoExplorer can be performed. The system is logically coherent and can be used together with other software tools like Microsoft Excel.

Fig. 2 presents exemplary SEM images of membranes enhanced by the MeMoExplorer: before (Ia) and after (IIa) hydrolysis. The images Ib and IIb present the corresponding graphs of areas of pores detected within the fixed size-ranges: 0–3, 3–8, 8–20, 20–80, 80–100, 100–150, 150–300, and 300  $\mu\text{m}^2$ , related to the total image surface.

Evaluation of the images Ia and IIa firstly revealed a nonhomogeneity of a spatial distribution of the small and large pores. This suggested that full images should have not been compared, but rather selected segments taken from the corresponding layers of the membrane sections would be preferred. Fig. 3 presents segments of SEM images of three examined membranes (PSf-PUR-1, PSf-PUR-2, and PSf-PUR-3) before (I) and after (II) hydrolysis.

A comparison of the effects of hydrolysis should be based on the statistics of the size of pores before and after the operation. For this purpose the following parameters were considered:

- Mean total areas  $m$  of pores in the image segments, calculated for (a) the given size-ranges, (b) all types of membranes, and (c) before ( $m_I$ ) and after ( $m_{II}$ ) hydrolysis;
- Standard deviations  $d$  of the total areas of pores, calculated for the above-mentioned cases in (1);

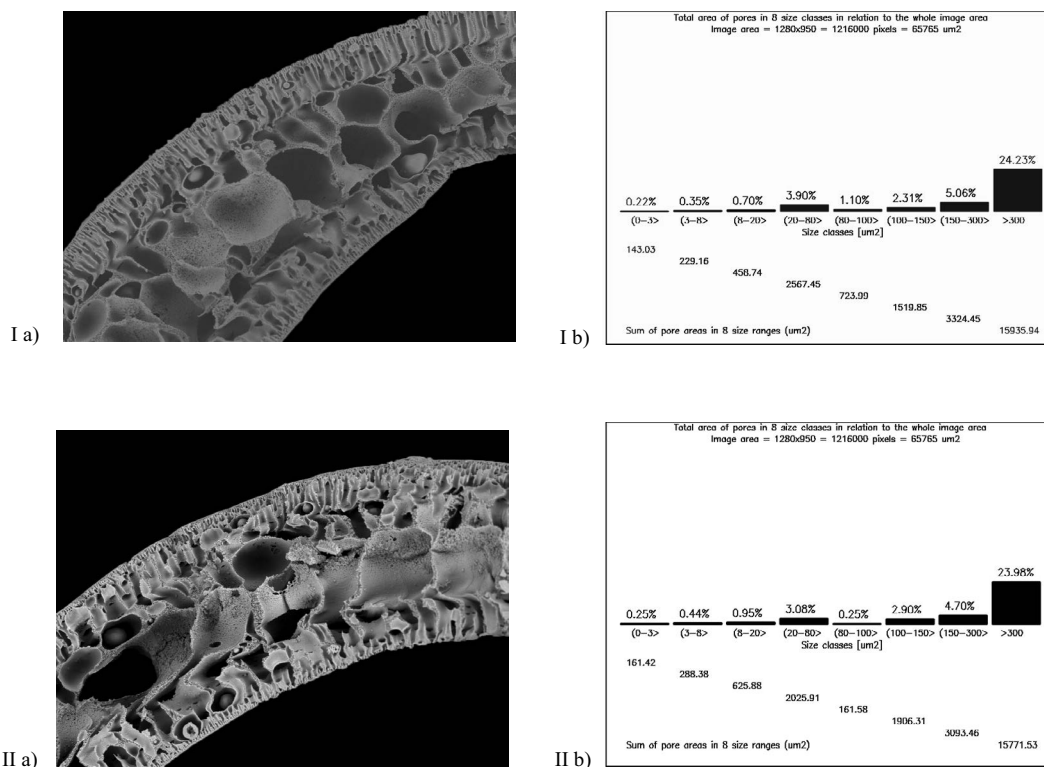


Fig. 2. Exemplary SEM images of membranes (Ia, IIa), the images (Ib, IIb) present the corresponding graphs of summarized pore areas in 8 size-ranges ( $\mu\text{m}^2$ ).

- Differences  $e$  between the mean values before and after hydrolysis, calculated for (a) the given size-ranges and (b) all types of membranes;
- Mean geometric (square root of a product) standard deviations  $D$  of the total areas of pores before and after hydrolysis, calculated for all types of membranes.
- Dissimilarity coefficient  $e$  of membrane porosity before and after hydrolysis, calculated for all types of membranes, according to the following formula:

$$e = \frac{m_I - m_{II}}{\sqrt{d_{II} \times d_{II}}} \quad (3)$$

The so-defined dissimilarity coefficient  $e$  for  $m_I$ ,  $m_{II}$  streaming to Gaussian distribution becomes a random value subjected to the second degree of the freedom Student probability distribution.

### 3. Results and discussion

#### 3.1. Membranes' mass measurements

The membranes' masses were evaluated before and after hydrolysis for checking what was the impact of NaOH hydrolysis on the membrane. PUR's mass shares ranged from 10% to 30% of the total membranes mass in modules. The measurements were repeated twice for each PSf/PUR

membrane. The results of PUR's mass changes are shown in Table 1.

The loss of PUR was observed in all types of PSf-PUR membranes. The loss differences in PUR's mass in all types of membranes were different and range from 25 to 80 of weight percentage. It indicated that the PUR was effectively removed from the membrane's structure and could act as a pore former. The amount of lost PUR declined with the increase of initial PUR's content. Differences in the mass loss of PUR could depend on time and kinetics of the hydrolysis. All types of membranes were hydrolyzed for the same period of time (48 h), but the membranes differed in the content of PUR. If the time of hydrolysis had been longer for the PSf-PUR-3 membrane, more PUR would have been removed.

#### 3.2. Membranes' hydraulic permeability (UFC)

The hydraulic permeability was measured (according to the Eq. (1)) before and after hydrolysis. The received values are presented in Table 2.

The coefficients of hydraulic permeability of PSf-PUR membranes before hydrolysis varied from 0.008 to 0.590 cm<sup>3</sup>/min m<sup>2</sup> hPa. It was caused by different amounts of the PUR. Membranes' UFC after hydrolysis increased from 1.95 to 2.68 cm<sup>3</sup>/min m<sup>2</sup> hPa and this could have been a result of PUR partial removal from the membranes. The higher amount

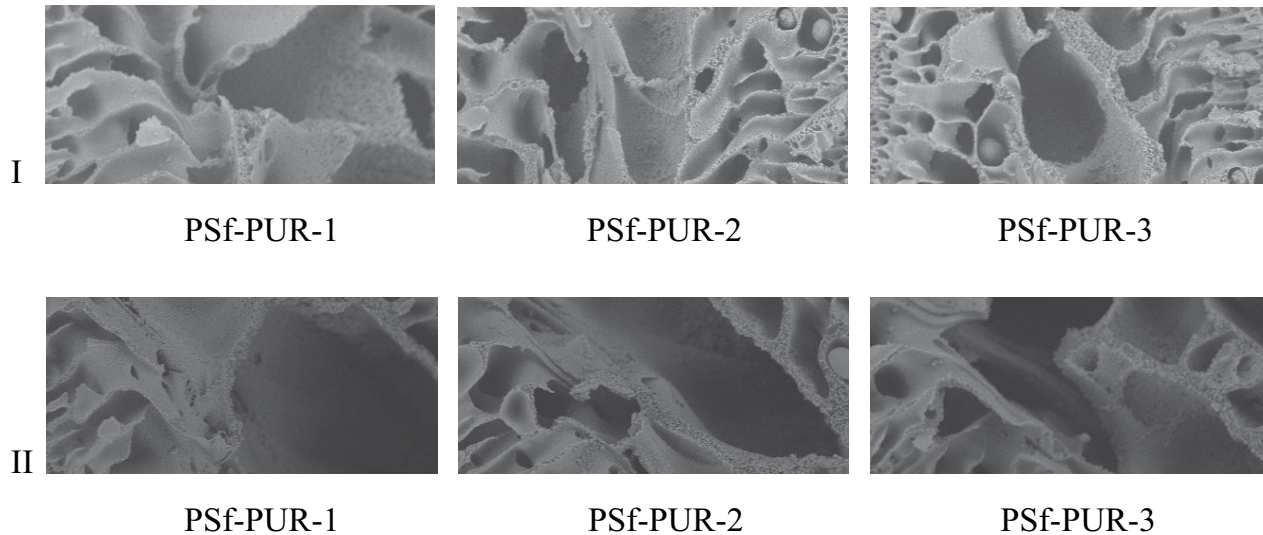


Fig. 3. Segments of SEM images of three examined membranes (PSf-PUR-1, PSf-PUR-2, and PSf-PUR-3) before (I) and after (II) hydrolysis.

Table 1  
The results of PUR's mass changes

Membrane	Membrane's mass before hydrolysis (g)	PUR's mass before hydrolysis (g)	PUR's mass loss after hydrolysis (g)	PUR's mass loss after hydrolysis (%)
PSf-PUR-1	0.0900	0.0090	0.0072	80
PSf-PUR-2	0.0900	0.0180	0.0082	45
PSf-PUR-3	0.0900	0.0270	0.0068	25

Table 2  
Coefficients of UFC for membranes before and after hydrolysis

Membrane	UFC before hydrolysis (cm <sup>3</sup> /min m <sup>2</sup> hPa)	UFC after hydrolysis (cm <sup>3</sup> /min m <sup>2</sup> hPa)	$\frac{\text{UFC after hydrolysis}}{\text{UFC before hydrolysis}}$
PSf-PUR-1	0.008	1.95	243.8
PSf-PUR-2	0.087	2.00	23.0
PSf-PUR-3	0.590	2.68	4.5

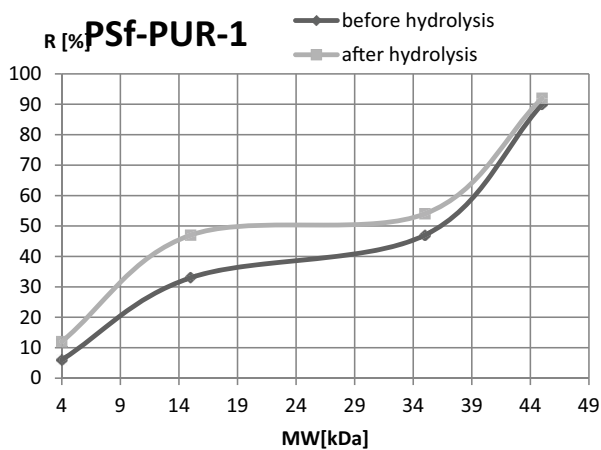


Fig. 4. Retention coefficient values for different markers for PSf-PUR-1 membrane before and after hydrolysis.

of washed PUR resulted in the increase of the coefficient of hydraulic permeability. The removal of PUR created the higher pores void volume of membrane that was shown in the figures (3 II; 8; 10; 12).

### 3.3. Membranes retention coefficients

The membrane's retention coefficients ( $R$ ) were evaluated before and after hydrolysis for different markers of particular M.W.: PEG 4, 15, and 35 kDa, CEA 45 kDa and BSA 67 kDa and are shown in Figs. 4–6.

The retention values after hydrolysis were higher than the values before hydrolysis. There were small differences for 4 kDa marker for all types of membranes and 45 kDa marker for PSf-PUR-1 and PSf-PUR-2 membranes. The highest differences in the retention values were observed for PSf-PUR-2 for 15 and 35 kDa markers. The smallest retention values differences in all types of markers were for the PSf-PUR-1 membrane with the lowest content of PUR. It was also observed that the hydrolysis had no influence on the membrane's cut-off. Consequently, the hydrolysis did not change the separation parameters of the membrane.

### 3.4. SEM of membranes

The PSf-PUR membranes' cross sections micrographs before hydrolysis are presented in Figs. 7(a) and (b); 9(a) and (b); 11(a) and (b) and after hydrolysis in Figs. 8(a) and (b); 10(a) and (b); 12(a) and (b).

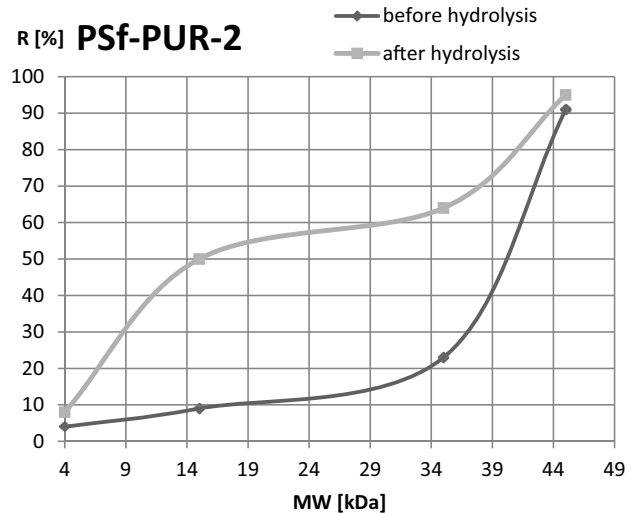


Fig. 5. Retention coefficient values for different markers for PSf-PUR-2 membrane before and after hydrolysis.

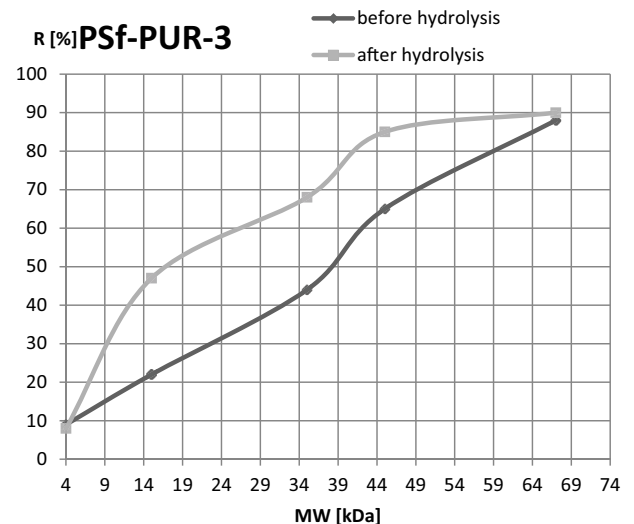


Fig. 6. Retention coefficient values for different markers for PSf-PUR-3 membrane before and after hydrolysis.

The result of hydrolysis was the removal of a part of the PUR from the membranes. In the membranes after hydrolysis pores were more dispersed and bigger than pores before hydrolysis. The hydrolysis process did not affect walls and diameters of the membranes.

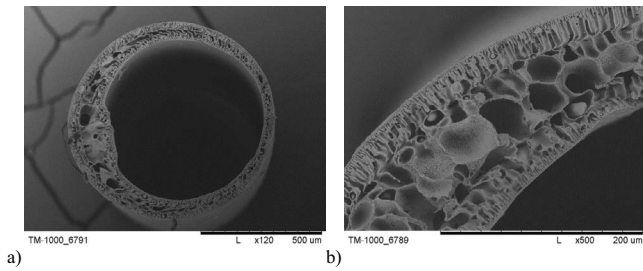


Fig. 7. Cross-section (a) and part of cross-section (b) of PSf-PUR-1 membrane before hydrolysis.

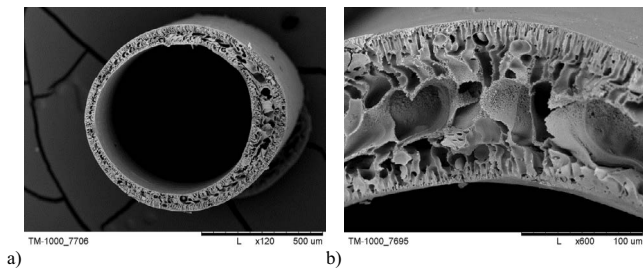


Fig. 8. Cross-section (a) and part of cross section (b) of PSf-PUR-1 membrane after hydrolysis.

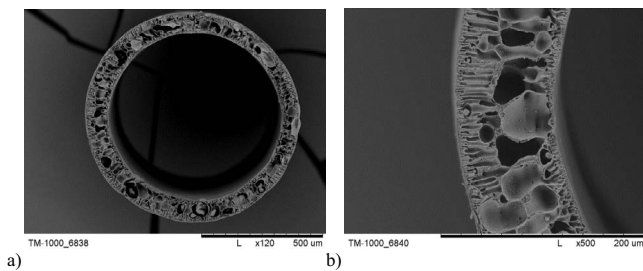


Fig. 9. Cross-section (a) and part of cross-section (b) of PSf-PUR-2 membrane before hydrolysis.

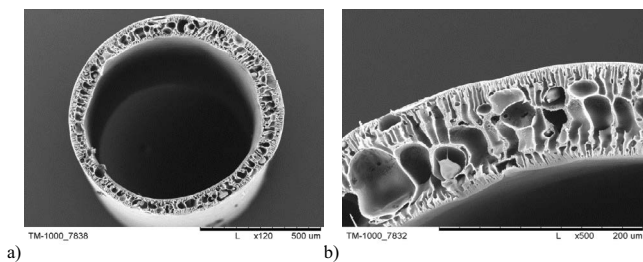


Fig. 10. Cross-section (a) and part of cross-section (b) of PSf-PUR-2 membrane after hydrolysis.

### 3.5. Comparative evaluation of porosity in membranes subjected to hydrolysis

The basic morphological parameters such as the size of pores of the membranes were tested by computer analysis of images. Coefficients of dissimilarity between membranes before and after hydrolysis for different sizes of pores are presented in Table 3.

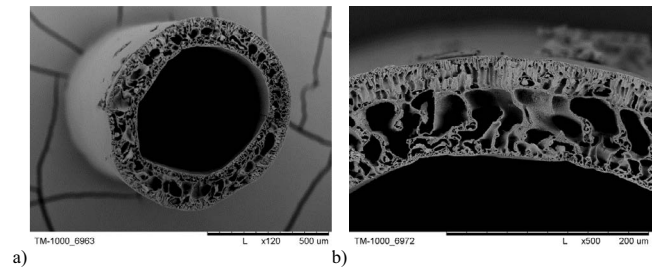


Fig. 11. Cross-section (a) and part of cross-section (b) of PSf-PUR-3 membrane before hydrolysis.

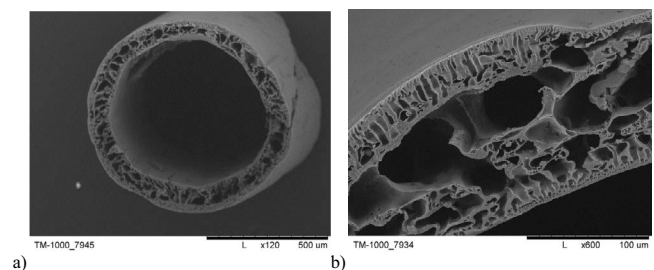


Fig. 12. Cross-section (a) and part of cross-section (b) of PSf-PUR-3 membrane after hydrolysis.

These differences between pores' sizes are also presented in Fig. 13.

Zero dissimilarity means no effect of hydrolysis. Fig. 13 presents collected results of evaluation of dissimilarity in 8 size-ranges in 3 different membranes. It can be observed that the membrane #1 was the least susceptible to hydrolysis. Moreover, the results corresponding to the highest (>300 nm<sup>2</sup>) size-range were less credible because they concerned large nonfully visible pores, canceled by the frames of the images.

The coefficients of dissimilarity between pores' sizes of the membrane before and after hydrolysis show that the hydrolysis process had an influence on morphological parameters of the membrane.

## 4. Conclusions

The target of this study was to obtain PSf-PUR blend hollow fiber membranes. The membranes should have been partially degradable and asymmetric. Three types of the PSf-PUR membranes were received in different weight proportion, in the process of phase inversion. The contents of PUR were 10%, 20%, and 30%. The PUR polymer contained degradable ester bonds. All types of PSf-PUR membranes were treated with 1 M NaOH water solution using the flowing method. PUR polymer was partly removed from the membranes as a result of the hydrolysis process. Mass measurements of the membranes before and after hydrolysis verified removal of PUR from the membranes (from 25% to 80% of PUR's weight).

The SEM images showed differences in structure of pores before and after the hydrolysis process. The structures and morphology of the membranes after hydrolysis were more porous. These differences were confirmed by the dissimilarity coefficient. The values of the dissimilarity coefficients were higher than zero.

Table 3  
Coefficients of dissimilarity of pores' sizes before and after hydrolysis

Pores' sizes ( $\mu\text{m}$ )	3	8	20	80	100	150	300	>300
PSf-PUR-1	0.27	0.11	0.04	0.34	0.15	0.49	0.04	0.20
PSf-PUR-2	1.07	0.60	0.28	0.27	0.42	0.11	0.34	1.29
PSf-PUR-3	0.91	0.20	0.35	1.05	0.01	0.73	0.13	0.69

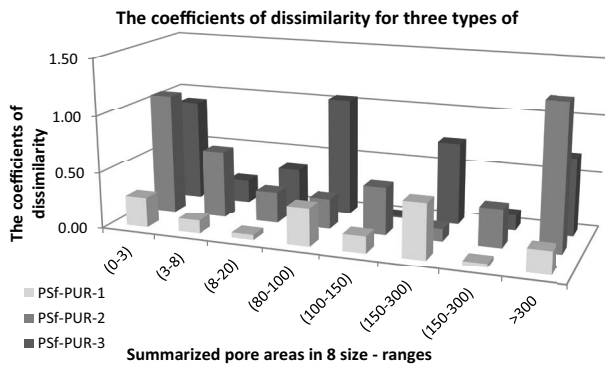


Fig. 13. Differences between pores' sizes of the membranes before and after hydrolysis.

The coefficients of hydraulic permeability (UFC) after hydrolysis increased from 0.008 to 1.95  $\text{cm}^3/\text{min m}^2 \text{ hPa}$  (for PSf-PUR-1); from 0.087 to 2.00  $\text{cm}^3/\text{min m}^2 \text{ hPa}$  (for PSf-PUR-2) and from 0.590 to 243.8  $\text{cm}^3/\text{min m}^2 \text{ hPa}$  (for PSf-PUR-3). For all types of membranes, the values of the membranes' retention were higher or the same (4 kDa for PSf-PUR-3, 45 kDa for PSf-PUR1, and 67 kDa for PSf-PUR-3) after hydrolysis for all types of markers. The differences were significant and showed the changes in the morphology of the membranes.

The higher retention coefficients for all types of the membranes after the hydrolysis were a serious surprise for us. We suppose that the partial hydrolysis caused the formation of polar groups or the partial removal of PUR increased the hydrophobicity of the membranes. These groups could cause better sorption of the polar markers. We hope that after complete hydrolysis the retention coefficients will be lower than the retention coefficients before hydrolysis.

PUR polymer was applied as a pore former in order to increase membrane porosity and recompense fouling. Changes of porosity caused the increase of the permeability of membranes. The PSf-PUR membranes after hydrolysis and partial removal of PUR were characterized by higher porosity, higher retention with no change in the molecular weight cut-off. Laboratory methods and computer analysis confirmed expressly the differences in the morphology of the membranes before and after hydrolysis.

The duration of membrane process is very important because regeneration or replacement of membranes during the process is very complicated or often impossible.

## References

- [1] B.S. Lalia, V. Kochkodan, R. Hashaikeh, N. Hilal, A review on membrane fabrication: structure, properties and performance relationship, *Desalination*, 326 (2013) 77–95.
- [2] I. Cabasso, E. Klein, J.K. Smith, Polysulfone hollow fibers. I. Spinning and properties, *J. Appl. Polym. Sci.*, 20 (1976) 2377–2394.
- [3] K. Rodemann, E. Staude, Synthesis and characterization of affinity membranes made from polysulfone, *J. Membr. Sci.*, 88 (1994) 271–278.
- [4] H. Ohya, S. Shiki, H. Kawakami, Fabrication study of polysulfone hollow-fiber microfiltration membranes: optimal dope viscosity for nucleation and growth, *J. Membr. Sci.*, 326 (2009) 293–302.
- [5] D.S. Kim, J.S. Kang, Y.N. Lee, The influence of membrane surface properties on fouling in a membrane bioreactor for wastewater treatment, *Sep. Sci. Technol.*, 39 (2005) 833–854.
- [6] R.E. Unger, K. Peters, Q. Huang, A. Funk, D. Paul, C.J. Kirkpatrick, Vascularization and gene regulation of human endothelial cells growing on porous polyethersulfone (PES) hollow fiber membranes, *Biomaterials*, 26 (2005) 3461–3469.
- [7] A.J. Brown, N.A. Brunelli, K. Eum, F. Rashidi, J.R. Johnson, W.J. Koros, C.W. Jones, S. Nair, Interfacial microfluidic processing of metal-organic framework hollow fiber membranes, *Science*, 345 (2014) 72–75.
- [8] L.M. Flendrig, A.A. te Velde, A.F.M. Chamuleau, Semipermeable hollow fiber membranes in hepatocyte bioreactors: a prerequisite for a successful bioartificial liver? *Artif. Organs*, 21 (1997) 1177–1181.
- [9] R.E. Unger, Q. Huang, K. Peters, D. Protzer, D. Paul, C.J. Kirkpatrick, Growth of human cells on polyethersulfone (PES) hollow fiber membranes, *Biomaterials*, 26 (2005) 1877–1884.
- [10] J.M. Schakenraad, J.A. Oosterbaan, P. Nieuwenhuis, I. Molenaar, J. Olijslager, W. Portman, M.J.D. Eenink, F. Feijen, Biodegradable hollow fibres for the controlled release of drugs, *Biomaterials*, 9 (1988) 116–120.
- [11] C. Charcosset, Z. Su, S. Karoor, G. Daun, C.K. Colton, Protein A immunoaffinity hollow fiber membranes for immunoglobulin G purification: experimental characterization, *Biotechnol. Bioeng.*, 48 (1995) 415–427.
- [12] H.J. Eash, H.M. Jones, B.G. Hattler, W.J. Federspiel, Evaluation of plasma resistant hollow fiber membranes for artificial lungs, *ASAIO J.*, 50 (2004) 491–497.
- [13] S.H. Ye, J. Watanabe, Y. Iwasaki, K. Ishihara, In situ modification on cellulose acetate hollow fiber membrane modified with phospholipid polymer for biomedical application, *J. Membr. Sci.*, 249 (2005) 133–141.
- [14] S. Luque, H. Mallubhotla, G. Gehlert, R. Kuriyel, S. Dzengeleski, S. Pearl, G. Belfort, A new coiled hollow-fiber module design for enhanced microfiltration performance in biotechnology, *Biotechnol. Bioeng.*, 65 (1999) 247–257.
- [15] K. Saito, Charged polymer brush grafted onto porous hollow-fiber membrane improves separation and reaction in biotechnology, *Sep. Sci. Technol.*, 37 (2002) 535–554.
- [16] S.P. Hong, T.H. Bae, T.M. Tak, S. Hong, A. Randall, Fouling control in activated sludge submerged hollow fiber membrane bioreactor, *Desalination*, 143 (2002) 219–228.
- [17] L.Y. Yu, Z.-L. Xu, H.-M. Shen, H. Yang, Preparation and characterization of PFDf-SiO<sub>2</sub> composite hollow fiber membrane by sol-gel method, *J. Membr. Sci.*, 337 (2009) 257–265.
- [18] Y. Hu, Z. Lü, C. Wei, S. Yu, M. Liu, C. Gao, Separation and antifouling properties of hydrolyzed PAN hybrid membranes prepared via in-situ sol-gel SiO<sub>2</sub> nanoparticles growth, *J. Membr. Sci.*, 545 (2018) 250–258.

- [19] X. Zhao, Y. Su, W. Chen, J. Peng, Z. Jiang, Grafting perfluoroalkyl groups onto polyacrylonitrile membrane surface for improved fouling release property, *J. Membr. Sci.*, 415–416 (2012) 824–834.
- [20] N.L. Le, M. Ulbricht, S.P. Nunes, How do polyethylene glycol and poly(sulfobetaine) hydrogel layers on ultrafiltration membranes minimize fouling and stay stable in cleaning chemicals? *Ind. Eng. Chem. Res.*, 56 (2017) 6785–6795.
- [21] S. Belfer, Modification of ultrafiltration polyacrylonitrile membranes by sequential grafting of oppositely charged monomers: pH-dependent behavior of the modified membranes, *React. Funct. Polym.*, 54 (2003) 155–165.
- [22] Y. Xie, S.-S. Li, X. Jiang, T. Xiang, R. Wang, C.-S. Zhao, Zwitterionic glycosyl modified polyethersulfone membranes with enhanced anti-fouling property and blood compatibility, *J. Colloid Interface Sci.*, 443 (2015) 36–44.
- [23] J.H. Kim, K.H. Lee, Effect of PEG additive on membrane formation by phase inversion, *J. Membr. Sci.*, 138 (1998) 153–163.
- [24] Y.-F. Zhao, L.-P. Zhu, Z. Yi, B.-K. Zhu, Y.-Y. Xu, Improving the hydrophilicity and fouling-resistance of polysulfone ultrafiltration membranes via surface zwitterionization mediated by polysulfone-based triblock copolymer, *J. Membr. Sci.*, 440 (2013) 40–47.
- [25] F. Pan, H. Jia, Z. Jiang, X. Zheng, J. Wang, L. Cui, P(AA-AMPS)-PVA/polysulfone composite hollow fiber membranes for propylene dehumidification, *J. Membr. Sci.*, 323 (2008) 395–403.
- [26] Y. Wan, H. Wu, A. Yu, D. Wen, Biodegradable polylactide/chitosan blend membranes, *Biomacromolecules*, 7 (2006) 1362–1372.
- [27] C. Wang, K.-W. Yan, Y.-D. Lin, P.C.H. Hsieh, Biodegradable core/shell fibers by coaxial electrospinning: processing, fiber characterization, and its application in sustained drug release, *Macromolecules*, 43 (2010) 6389–6397.
- [28] U.H. Khan, Z. Khan, I.H. Aljundi, Improved hydrophilicity and anti-fouling properties of polyamide TFN membrane comprising carbide derived carbon, *Desalination*, 420 (2017) 125–135.
- [29] P. Aerts, I. Genne, S. Kuypers, R. Leysen, I.F.J. Vankelecom, P.A. Jacobs, Polysulfone-aerosil composite membranes: Part 2. The influence of the addition of aerosol on the skin characteristics and membrane properties, *J. Membr. Sci.*, 178 (2000) 1–11.
- [30] S.H. Yoo, Y.H. Kim, Y.H. Yho, J. Won, Y.S. Kang, Influence of the addition of PVP on the morphology of asymmetric polyimide phase inversion membranes: effect of PVP molecular weight, *J. Membr. Sci.*, 236 (2004) 203–207.
- [31] B. Chakrabarty, A.K. Ghoshal, M.K. Purkait, Preparation, characterization and performance studies of polysulfone membranes using PVP as an additive, *J. Membr. Sci.*, 315 (2008) 36–47.
- [32] R. Mahendran, R. Malaisamy, D.R. Mohan, Cellulose acetate and polyethersulfone blend ultrafiltration membranes. Part I: preparation and characterizations, *Polym. Adv. Technol.*, 15 (2004) 149–157.
- [33] C. Wojciechowski, A. Chwojnowski, L. Granicka, E. Łukowska, Polysulfone/cellulose acetate blend semi degradable capillary membranes preparation and characterization, *Desal. Wat. Treat.*, 64 (2017) 365–371.
- [34] C. Wojciechowski, A. Chwojnowski, L. Granicka, E. Łukowska, M. Grzechkiewicz, Polysulfone/polyurethane blend degradable hollow fiber membranes preparation and transport-separation properties evaluation, *Desal. Wat. Treat.*, 57 (2016) 22191–22199.
- [35] M. Przytułska, A. Kruk, J.L. Kulikowski, C. Wojciechowski, A. Gadomska-Gajadur, A. Chwojnowski, Comparative assessment of polyvinylpyrrolidone type of membranes based on porosity analysis, *Desal. Wat. Treat.*, 75 (2017) 18–25.
- [36] M. Przytułska, J.L. Kulikowski, M. Wasyleczko, A. Chwojnowski, D. Piętka, The evaluation of 3D morphological structure of porous membranes based on a computer-aided analysis of their 2D images, *Desal. Wat. Treat.* (2018) 1–9, doi:10.5004/dwt.2018.22569.